Optical Coding for Next-Generation Survivable Long-Reach Passive Optical Networks

Maged Abdullah Esmail and Habib Fathallah

***Abstract*—Optical coding has been proposed and has been well investigated for the monitoring of standard time domain multiplexing passive optical networks (TDM-PONs). We propose a physical layer fault management and protection system for next-generation passive optical networks, so-called long-reach PON (LR-PON), based on passive optical coding. Our approach exploits adapted, performance enhanced, and inexpensive passive optical components in the field, and electronic switches in the central office (CO). This allows detection and localization of the faulty segments in addition to the faulty nodes, hence decreasing the false alarm probability encountered in previous proposed approaches. We show that ring duplication protection in LR-PON can save almost half the cost compared with full duplication protection, with relatively high availability (99.992%). We describe the implementation strategy of our system in various well-known metro network topologies, including (1) single-ring-, (2) double-ring-, and (3) double-fiber-pairs-based ring topologies; all are considered different varieties of ring-and-spur LR-PON. The internal architecture of the remote nodes and the CO are also described in addition to the appropriate placement of our passive monitors. We develop two novel symmetric coding settings. We call them symmetrical optical encoders, which are suitable for fault detection and localization in the ring. We also develop the algorithms required to be executed by the network management system in the CO for fault detection, localization, and protection. Expressions for the upper bound notification and recovery times are also derived. Finally, we estimate that our system can recover from a fault in less than 0.5 ms for a 100 km ring length.**

***Index Terms*—Fault detection; Fault management; Long-reach PON; Network protection; Optical encoder; Recovery time.**

I. Introduction

The long-reach passive optical network (LR-PON) is considered a potential cost-effective solution for next-generation broadband optical access networks. LR-PON extends the PON coverage from the traditional 20 km span to 100 km and beyond. This large coverage area supports more customers by exploiting wavelength division multiplexing (WDM) technology [1,2]. Figure 1 illustrates the general architecture of the WDM/time domain multiplexing (TDM) LR-PON, the so-called ring-and-spur topology [3,4]. The network consists of a feeder section (ring), a distribution section, and a drop section in a tree structure. The ring section connects the optical line terminal (OLT) located in the central office (CO) to a number of remote nodes (RNs) by optical fibers, forming a physical ring topology. The distribution section runs from the RN to the power splitter/combiner (PSC). The drop section runs from the PSC to the optical network units (ONUs).

The downstream data in the waveband Λ_D (for example, C band) are transmitted from the CO in the counterclockwise direction. At RN_i, subwaveband Λ_i, which may include one or more wavelength(s), is demultiplexed and dropped to the access network. The dropped subwaveband is split and sent to each ONU in the access network. The upstream subwaveband from the access network will be added and multiplexed in RN_i and then transmitted in the counterclockwise direction.

This network can carry huge amounts of data (up to Tbit/s). It supports a high number of customers and covers a large area. Any fault in the network physical layer, especially the ring, will cause high data loss, customer dissatisfaction, and complaints. The network operator should respect the service level agreement to gain customer satisfaction and improve the network's business. Hence, an efficient management system for fault detection and protection is highly required. This system should be intelligent and cost-effective and have a short fault recovery time.

Network survivability has attracted more attention over the most recent few years. Most of the conventional approaches of fault management in optical networks rely on diagnosis in higher layers, based on status reports collected from various checkpoints on the managed optical networks. However, this would impose excessive overhead in network signaling as well as in the network management system (NMS). Moreover, an upper layer protocol often requires a much longer detection time than a physical layer technique. Therefore, fault detection is recommended to take place at the layer closest to the fault, which is the physical layer for optical networks [5]. This facilitates network protection and restoration.

In this paper, we propose a management system that uses passive components in the field. This system can identify and localize faults in the ring and then notify the CO to initiate

Manuscript received May 15, 2012; revised October 17, 2012; accepted October 18, 2012; published November 30, 2012 (Doc. ID 168665).

Maged Abdullah Esmail (e-mail: abdullahmaged@gmail.com) is with the Electrical Engineering Department, King Saud University, Saudi Arabia, and he is also with the Prince Sultan Advanced Technologies Research Institute (PSATRI) and Saudi Telecommunication Company (STC), Saudi Arabia.

Habib Fathallah is with the Electrical Engineering Department, King Saud University, Saudi Arabia, and he is also with the Prince Sultan Advanced Technologies Research Institute (PSATRI) and Saudi Telecommunication Company (STC), Saudi Arabia, and he is also with the Electrical and Computer Engineering Department, Laval University, Quebec, Canada.

Digital Object Identifier 10.1364/JOCN.4.001062

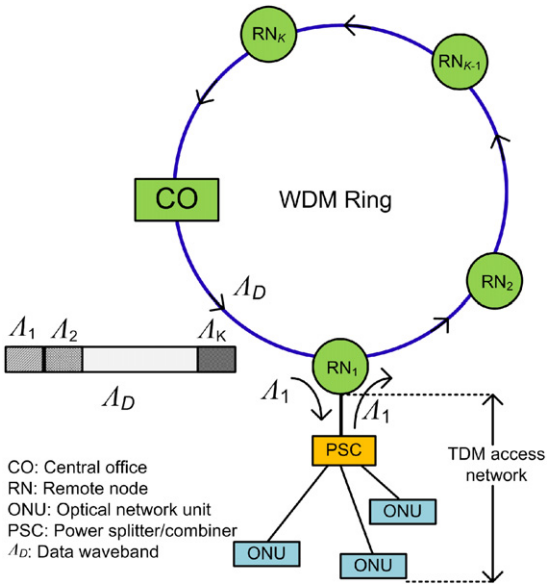

Fig. 1. (Color online) Ring-and-spur LR-PON architecture.

the protection process. The system has a short recovery time, about 0.5 ms, as an upper bound. Compared with previous approaches in [6,7] that use active components in the RN (intelligent RNs), our system uses passive components for the monitoring. Hence it reduces the capital and operational expenditures, as no electronic devices are used. The proposed system is centralized in that the fault detection is achieved by the NMS in the CO rather than using monitors or detectors in the RN.

Using passive components in the field to prevent ring failure is reported in [8,9]. These approaches detect a fault based on monitoring the upstream data wavelengths in the CO. However, this reported detection can lead to a false alarm. For example, a fault in RN$_i$ will cause loss for upstream subwaveband Λ_i from RN$_i$. When the CO detects this miss, it will interpret it as a fault in the ring segment between RN$_i$ and RN$_{i+1}$. This leads to unwanted activation of the protection mechanism, hence increasing the operational expenditures by dispatching technicians to fix a fault in the wrong location. Our system overcomes this issue by also monitoring the RNs, not only the ring segments. Another scenario for false alarm that is generated with other reported approaches occurs when the distribution fiber (DF) between the RN and the PSC is faulty. This causes misdetection for the upstream signal that leads to false alarm. Our system avoids this, since it does not depend on the upstream signals to detect the status of the physical layer.

In Section II, we study the network availability and cost for different well-known protection networks. We show that LR-PON protection by ring duplication has high availability with lower cost compared with other duplication protection schemes. In Sections III and IV, we respectively describe different ring protection architectures and our NMS proposal. Physical layer fault detection, localization and protection algorithms are developed in Section V, and fault notification and recovery times are investigated and derived in Section VI. Finally, we conclude in Section VII.

II. Availability and Cost Analysis

To define the deployment strategy of our coding-based management system, in this section we address the link between fault monitoring and protection mechanisms. Any network management and protection system should take into account two critical factors: level of service availability and network cost. In the access part of the network, the economical aspects are most critical because of the low sharing factor of the network deployment and management cost. Hence, in this section we study these factors for four different architectures of ring-and-spur LR-PON. Figure 2 shows the availability models illustrated by availability block diagrams (ABDs) derived from the LR-PON shown in Fig. 1. The ABD is a representation method for all components in the network and how each component is connected [10]. Each device or component in the network is represented by a block. Figure 2(a) shows the basic network ABD without protection. The ABD includes all the optical components and devices in the signal path from the CO to the ONU. This includes the OLT equipment, the ring fiber (RF), the optical add–drop multiplexer (OADM, or generally we call it RN) at the RNs, the DF that connects the RN with the PSC, the PSC component, the distribution and drop fiber (DDF) that connects the PSC with the ONU, and finally the ONU equipment. Each component or device is represented by a box. Figure 2(b) shows the network ABD with the only duplication in the access network. In this ABD, an optical switch (OS) is used to select between one of the two access networks. Figure 2(c) shows the network with the duplicated ring, where two synchronous OSs are used to route the data through one of the two rings. Figure 2(d) represents the network ABD with full duplication. This network has two signal paths in the ring and two paths in the access network. Hence four paths are available for the data signal by using OSs to select any one of them. A failure occurs only when the connection (path) between the OLT and the ONU is interrupted owing to the failure of system components in this path. The system is working when at least one path runs from the OLT to the ONU.

By definition, the availability of a component/system is the proportion of time in which a system is providing its intended service or function, observed in the limit as time increases toward infinity [10]. The unavailability of component i (complement of availability) is derived from its mean time to repair (MTTR) given as

$$U_i = \text{MTTR} * \text{FITs}/10^9, \tag{1}$$

where FIT (failure in time) is a unit for measuring the failure rates. One FIT means one failure in 10^9 h [10]. For n components connected in series, the total unavailability $U_{\text{tot-series}}$ is

$$U_{\text{tot-series}} \approx \sum_{i=1}^{n} U_i, \tag{2}$$

whereas for n components connected in parallel, the total unavailability $U_{\text{tot-parallel}}$ is given as

$$U_{\text{tot-parallel}} = \prod_{i=1}^{n} U_i. \tag{3}$$

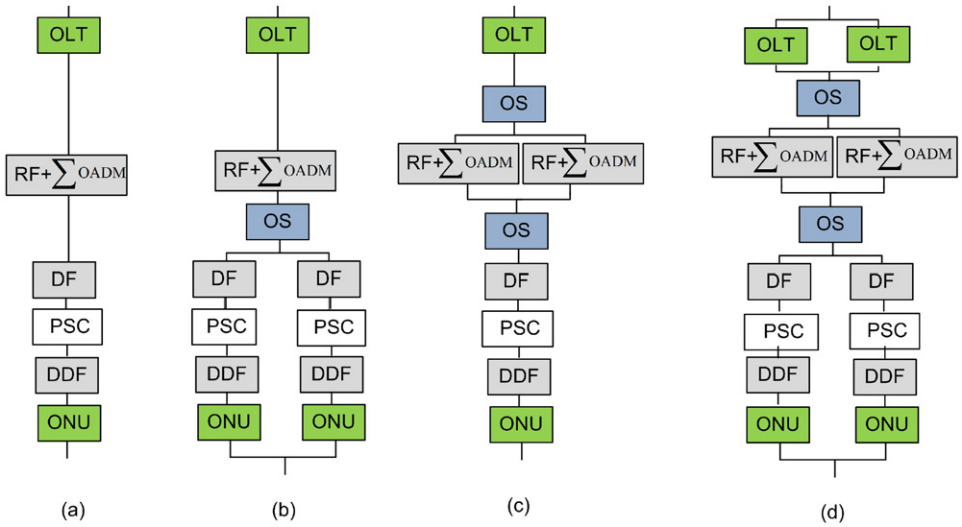

Fig. 2. (Color online) ABD for different LR-PON protection architectures.

Typical values of the FIT and MTTR of the various components involved in the system are obtained from [11,12] and reported in Table I. We have, however, updated their prices by using recent data. Note that the encoder shown in Table I is the basic element in our NMS. A detailed description for its design and operation will be given in Section IV. In our calculations, we assume that the ring feeder length is ($L_{\mathrm{RF}} = 100$ km) and that the distance between any RN and the farthest ONU at the user premises (the sum of DF and DDF) is 20 km. Moreover, we consider that there are 31 RNs ($K = 31$) with $N = 32$ ONUs in each TDM access network connected to the RN. The deployment scenario considered here is a dense populated area (collective). In this scenario, the length of DF is $L_{\mathrm{DF}} = 19.5$ km and the length of DDF is $L_{\mathrm{DDF}} = 0.5$ km. We also assume that the ONU in Fig. 2 is the one connected to the middle of the ring, i.e., $\mathrm{RN}_{(K+1)/2}$.

Using the assumptions above, the unavailability definition in Eqs. (2)–(3) and the symbols in Table I, we can derive the cost and unavailability expressions for each network architecture in Fig. 2.

A. Unprotected LR-PON

For the unprotected topology (Fig. 2(a)), only one path is available between the OLT and the customer; the network cost C_{UP} is derived as

$$C_{\mathrm{UP}} = C_{\mathrm{OLT}} + \underbrace{L_{\mathrm{RF}}(C_F + C_B) + KC_{\mathrm{OADM}}}_{\text{Ring}} + \underbrace{K[L_{\mathrm{DF}}(C_F + C_B)}_{\text{Access}}$$
$$\underbrace{+C_S + N(L_{\mathrm{DDF}}(C_F + C_B) + C_{\mathrm{ONU}}]}_{\text{Access}} + 64C_E, \quad (4)$$

where $C_{\mathrm{OLT}}, C_F, C_B, C_{\mathrm{OADM}}, C_S, C_{\mathrm{ONU}}$ and C_E represent the cost of the OLT, fiber, burying, OADM, splitter, ONU, and encoder, respectively. The unavailability U_{UP} of the network is

$$U_{\mathrm{UP}} = U_{\mathrm{OLT}} + \underbrace{L_{\mathrm{RF}}/2 * U_F + (K+1)/2 * U_{\mathrm{OADM}}}_{\text{Ring}}$$
$$\underbrace{+ U_S + (L_{\mathrm{DF}} + L_{\mathrm{DDF}}) * U_F + U_{\mathrm{ONU}}}_{\text{Access}}, \quad (5)$$

where U_{OLT}, U_F, U_{OADM}, U_s and U_{ONU} represent the unavailability of the OLT, fiber, OADM, splitter, and ONU, respectively.

B. Access-Only Protected LR-PON

When only the access segment of the LR-PON is protected, as shown in Fig. 2(b), the network cost C_{AP} is derived as

$$C_{\mathrm{AP}} = C_{\mathrm{OLT}} + \underbrace{L_{\mathrm{RF}}(C_F + C_B) + KC_{\mathrm{OADM}}}_{\text{Ring}} + KC_{\mathrm{OS}} + \underbrace{2K[L_{\mathrm{DF}}}_{\text{Access}}$$
$$\underbrace{*(C_F + C_B) + C_S + N(L_{\mathrm{DDF}}(C_F + C_B) + C_{\mathrm{ONU}})]}_{\text{Access}}$$
$$+ 64C_E, \quad (6)$$

where C_{OS} is the cost of the optical switch. The network unavailability U_{AP} is

$$U_{\mathrm{AP}} = U_{\mathrm{OLT}} + \underbrace{L_{\mathrm{RF}}/2 * U_F + (K+1)/2 * U_{\mathrm{OADM}}}_{\text{Ring}} + U_{\mathrm{OS}}$$
$$\underbrace{+ [U_S + (L_{\mathrm{DF}} + L_{\mathrm{DDF}}) * U_F + U_{\mathrm{ONU}}]^2}_{\text{Access}}, \quad (7)$$

where U_{OS} is the optical switch unavailability. We note that the cost of the access part of the network doubles while its unavailability decreases, compared with the unprotected network, because we have two available paths between the OLT and the customer.

TABLE I
COMPONENT UNAVAILABILITY AND COST

Component/Device	FIT	MTTR (H)	Unavailability		Cost ($)	
OLT	256	2	U_{OLT}	5.12E−07	C_{OLT}	500
ONU	256	2	U_{OLT}	5.12E−07	C_{ONU}	150
Splitter 1 × 32	50	2	U_S	1.00E−07	C_S	100
Optical switch	200	2	U_{OS}	4.00E−07	C_{OS}	80
OADM	200	2	U_{OADM}	4.00E−07	C_{OADM}	600
Fiber (/km)	570	6	U_F	3.42E−06	C_F	1.0
Burying Fibers (/km)					C_B	250
Encoder					C_E	50

C. Ring-Only Protected LR-PON

For ring protection architecture (Fig. 2(c)), the cost C_{RP} and unavailability U_{RP} are derived as

$$C_{RP} = C_{OLT} + C_{OS} + \underbrace{2[L_{RF}(C_F + C_B) + KC_{OADM}]}_{\text{Ring}} + KC_{OS} + \underbrace{K[L_{DF}(C_F + C_B) + C_S + N(L_{DDF}(C_F + C_B) + C_{ONU})]}_{\text{Access}} + 128C_E \quad (8)$$

and

$$U_{RP} = U_{OLT} + U_{OS} + \underbrace{[L_{RF}/2 * U_F + (K+1)/2 * U_{OADM}]^2}_{\text{Ring}} + U_{OS} + \underbrace{U_S + (L_{DF} + L_{DDF})U_F + U_{ONU}}_{\text{Access}}. \quad (9)$$

Equations (8)–(9) show that the network unavailability is decreased while its cost is increased.

D. Fully Protected LR-PON

Finally, for full network protection (Fig. 2(d)), the cost C_{FP} and unavailability U_{FP} are derived as

$$C_{FP} = 2C_{OLT} + C_{OS} + \underbrace{2[L_{RF}(C_F + C_B)] + 2KC_{OADM}}_{\text{Ring}} + KC_{OS} + \underbrace{2K[L_{DF}(C_F + C_B) + C_S) + N(L_{DDF}(C_F + C_B)}_{\text{Access}} \underbrace{+C_{ONU})]}_{\text{Access}} + 128C_E \quad (10)$$

and

$$U_{FP} = [U_{OLT}]^2 + U_{OS} + \underbrace{[L_{RF}/2 * U_F + (K+1)/2 * U_{OADM}]^2}_{\text{Ring}} + U_{OS} + \underbrace{[U_S + (L_{DF} + L_{DDF})U_F + U_{ONU}]^2}_{\text{Access}}. \quad (11)$$

Using Eqs. (4)–(11) and the values in Table I, the cost and availability of each network architecture is calculated and presented in Fig. 3. By comparing the different protection architectures with no protection, the results show that using access region duplication will increase the cost by 26% with small improvement in network availability (99.982%). The metro ring duplication has high availability, 99.992% (four nines), and small increment in the cost, 10.3%. The best availability is for the full protection network, 99.999% (five nines), but its cost increases approximately 100%. Hence, we see that ring protection has a reasonable increment in the cost with high availability (four nines) which is close to full protection (five nines).

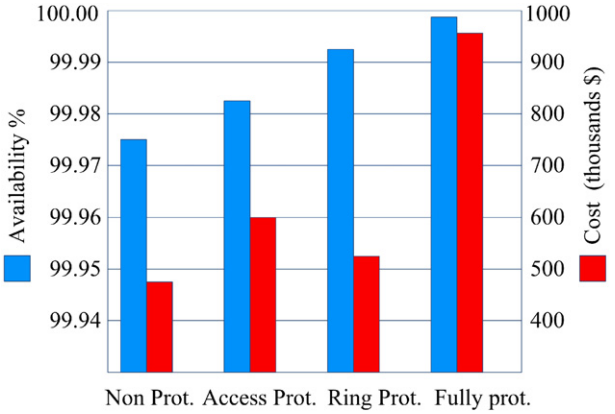

Fig. 3. (Color online) Availability and cost of different LR-PON protection architectures.

From these results for the availability and cost of the different protection architectures, it is clear that almost half the cost compared with that for full protection can be saved with high availability if only ring duplication protection is used. However, duplicating the ring is not enough when a fault management system is required to detect and localize the fault in the ring and then apply a suitable protection procedure. Therefore, in this paper, we propose a management system for fault detection, localization, and protection of the metro ring. This management system enables fast fault recovery by using passive devices in the field. In order to design an optical coding-based monitoring solution for ring networks, in the next section we address several ring architectures widely encountered in the literature.

III. METRO RING-BASED LR-PON PROTECTION ARCHITECTURES

Different widely used ring protection architectures exist in metro ring networks. Any deployment of LR-PON needs to

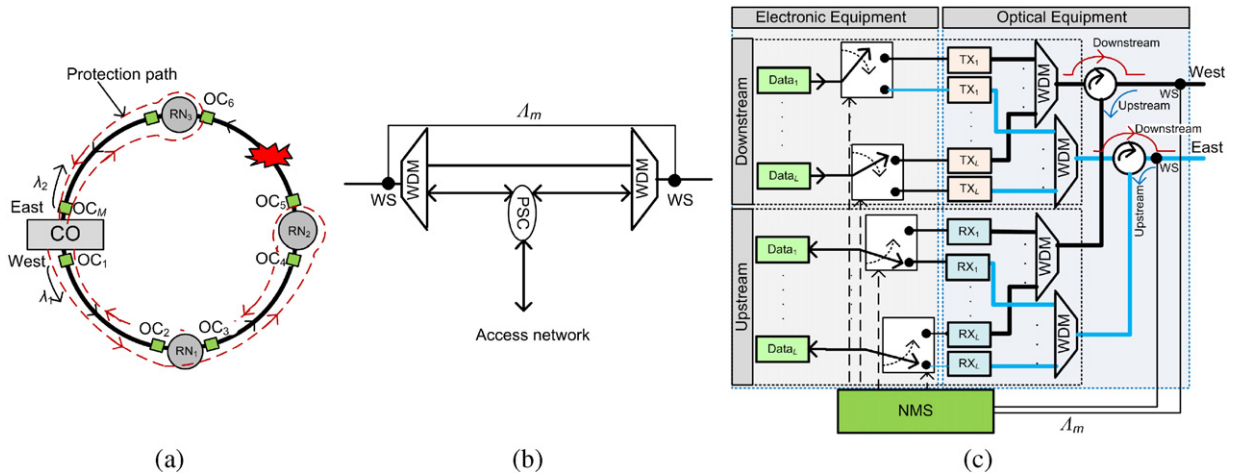

Fig. 4. (Color online) Single bidirectional LR-PON ring protection: (a) ring design (OCs shown in squares), (b) RN architecture, and (c) OLT architecture.

consider the specific constraint of each of these architectures. Consequently, an appropriate NMS should take into account most or all of these architectures in order to detect and localize the fault and then recover the network. As we will see in this and the next sections, our proposed NMS can be deployed in any ring-based architecture. This NMS is based on using passive optical encoders at the end of each fiber segment in the ring. A monitoring pulse that has a wavelength from the monitoring waveband (Λ_m) is transmitted to the ring. Then the optical encoders use this pulse to generate codes and reflect them to the NMS in the CO. The alarm that is generated by the NMS when an optical code (OC) is missed (fault occurred) is used to control the route of the data signal in the ring. In this section, we describe the key metro ring architectures. The NMS will be addressed in detail in Section IV.

A. Single Bidirectional Ring Protection

In the single bidirectional ring protection architecture, only one bidirectional ring is used for the downstream and upstream data signals. In normal mode (no fault), the downstream data signals are transmitted through the west as shown in Fig. 4(a). At each RN, a subwaveband is dropped. Recall that each subwaveband may contain one or a number of wavelengths that serve the respective area. The upstream signal from the access network is transmitted in both directions of the ring by the 3 dB PSC shown in Fig. 4(b). Hence, the 3 dB PSC provides a protection function, so that upstream data signals can be received either from west or east. The monitoring waveband (Λ_m) bypasses the RN as shown in Fig. 4(b) by using wavelength selectors (WSs). At the CO, the upstream signals from the east are chosen by switches shown in Fig. 4(c), whereas the upstream signals from the west are neglected. The circulators in Fig. 4(c) are used to route the downstream data signals to the ring and route the upstream data signals to the receivers.

When a fault occurs as shown in Fig. 4(a) between RN_2 and RN_3, the downstream data to RN_3 are lost. Also, the upstream data from RN_1 and RN_2 are lost. Once this fault is detected and localized in the CO by the NMS, an alarm is generated, and a signal is used to initiate the protection mode by controlling the operation of the switches as shown in Fig. 4(c). In protection mode, the downstream data for RN_1 and RN_2 are transmitted through the west, whereas the downstream data for RN_3 are transmitted through the east. For the upstream data, the switches are controlled to receive the upstream data from RN_1 and RN_2 on the west and that from RN_3 on the east.

In Fig. 4(c), we show the OLT implementation that uses electronic switches to select either the normal or the protection mode transmitters (TXs) and receivers (RXs). Note that this implementation requires $2L$ electronic switches, $2L$ TXs, and $2L$ RXs, where L is the number of wavelengths in the data waveband. If optical switches are used, we need $2L$ switches, L TXs, and L RXs. The cost of an electronic switch is quite negligible compared with that of optical switches. Also, the cost of an optical switch maybe considered close to that of a TX or RX, making the overall cost of both configurations almost the same. However, electronic switches are now available with high switching speeds, much better adapted for our application than optical switches. Hence, we suggested using electronic switches because they take a shorter time to switch to the protection mode; the recovery time is a critical factor in designing protection systems.

Figure 4(a) also shows the deployment strategy of our encoders (square boxes). One encoder is installed at the end of each fiber segment (OC_2, OC_4, etc.). To monitor the RN itself, we install another optical encoder behind each RN (OC_3, OC_4, etc.). This deployment strategy ensures detecting any fault in the physical layer. In normal mode operation, the NMS sends a monitoring signal from the west side and collects the fault information from the same side. In case of a fault, the NMS sends monitoring signals from both sides and then collects the fault information from both sides as well. This ensures detecting cases of two simultaneous faults. Specific encoder design that allows symmetric code generation from both sides (east and west) and NMS operation will be discussed in Section IV.

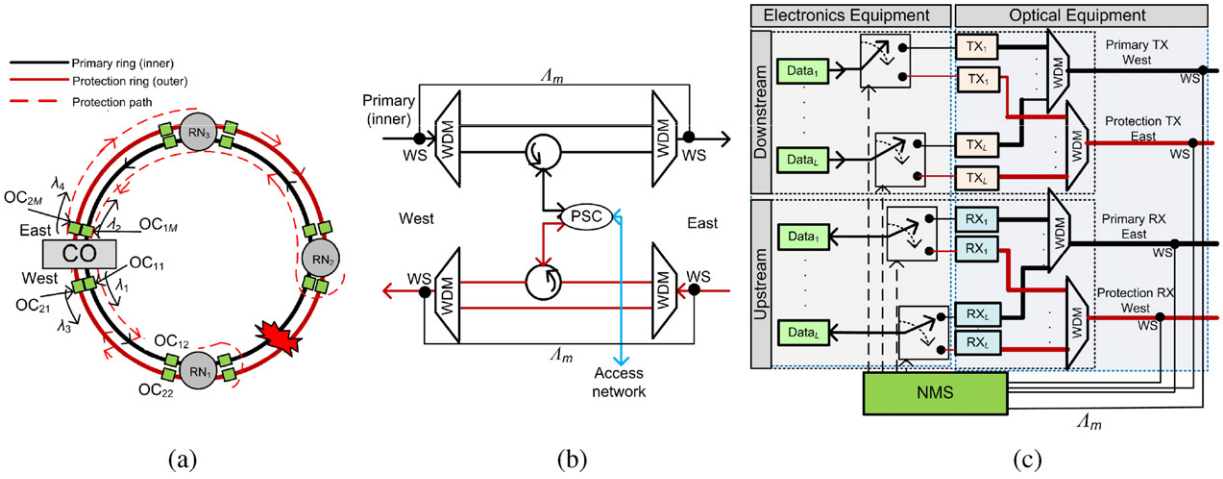

Fig. 5. (Color online) Double-ring LR-PON protection: (a) ring design (OCs shown in squares), (b) RN architecture, and (c) OLT architecture.

B. Double-Ring Protection

Although the single bidirectional ring protection can recover from a single fault in the ring, two faults in different segments of the ring will make the protection useless. Using two rings will solve this problem, as shown in Fig. 5(a); one ring is primary (inner ring), and one is for protection (outer ring). In normal mode, the OLT transmits data on the primary ring (west) and nothing is transmitted in the protection ring (east). The 3 dB coupler in the RN shown in Fig. 5(b) divides the upstream signals from the access network to both rings. In the primary ring, the multiplexed upstream signals will continue propagating in the counterclockwise direction toward the CO (east). In the protection ring, the multiplexed upstream signals take the clockwise direction toward the CO (west). Hence upstream signals can be received either from the primary or protection rings. The monitoring waveband (Λ_m) bypasses the RN by using wavelength selectors as shown in Fig. 5(b). At the CO, the signals received from the primary ring (east) are chosen by switches shown in Fig. 5(c), whereas the signals received from the protection ring (east) are neglected.

In protection mode we can define two scenarios of operation. The first scenario corresponds to single or multiple faults occurring in the primary ring. In this case, the NMS controls the switches to transmit and receive signals on the protection ring. The downstream data are transmitted on the protection ring (east), and the upstream data are received on the protection ring (west). The second scenario corresponds to faults that occur on both segments between two RNs. For example, Fig. 5(a) shows faults on both fibers in the segment between RN_1 and RN_2. In this case the downstream data to RN_2 and RN_3 are lost, and also the upstream data from RN_1. Once these faults are detected and localized in the CO by the NMS, an alarm is generated, and a control signal is applied to the switches. The downstream data for RN_1 are transmitted on the primary ring (west), whereas the downstream data for RN_2 and RN_3 are transmitted on the protection ring (east). For the upstream data, the switches are controlled to receive the upstream data from RN_1 on the protection ring (west) and the upstream data for RN_2 and RN_3 on the primary ring (east). The encoders' deployment strategy is similar to that of a single-ring network, but encoders are installed on both rings. The NMS sends monitoring signals depending on operation mode. For normal mode, a monitoring signal is transmitted from the west, and fault information is collected from the same side. For faults in the inner ring, a monitoring signal is transmitted from the east, and fault information is collected from east as well. If both rings are faulty, monitoring signals are transmitted from both sides, and fault information is collected from both sides as well. This ensures detecting up to four simultaneous faults, as we will see in Sections IV and V.

C. Double-Ring Pairs Protection

Similar to bidirectional line switched ring protection in SONET networks, the same principle of protection is applied for ring-and-spur LR-PON to increase the availability of the network. Figure 6(a) shows the protection architecture, where two ring pairs (inner and outer) are used. Each pair has primary and protection rings. This architecture can protect the network when there is more than double failure in the rings, as shown in Fig. 6(a), where the outer ring pair is faulty. In this case the inner pair is used. Another fault scenario is shown in Fig. 6(b), where a fault happens in the protection ring of the inner pair and the primary ring of the outer pair. In this case the NMS will use the primary of the inner pair and the protection of the outer pair to protect the network. The RN in this protection architecture, shown in Fig. 6(c), is duplication for the RN in Fig. 5(b) with extra 1×2 PSCs to combine the upstream and downstream signals for the access network. The number of encoders in this network is four times that used in the single bidirectional network. However, their cost is negligible compared with other components such as fiber installation.

D. Ring Protection Architectures Comparison

In Section II, we showed that the preferred protection architecture is ring duplication in the sense that it gives a good compromise between cost and availability. Then we

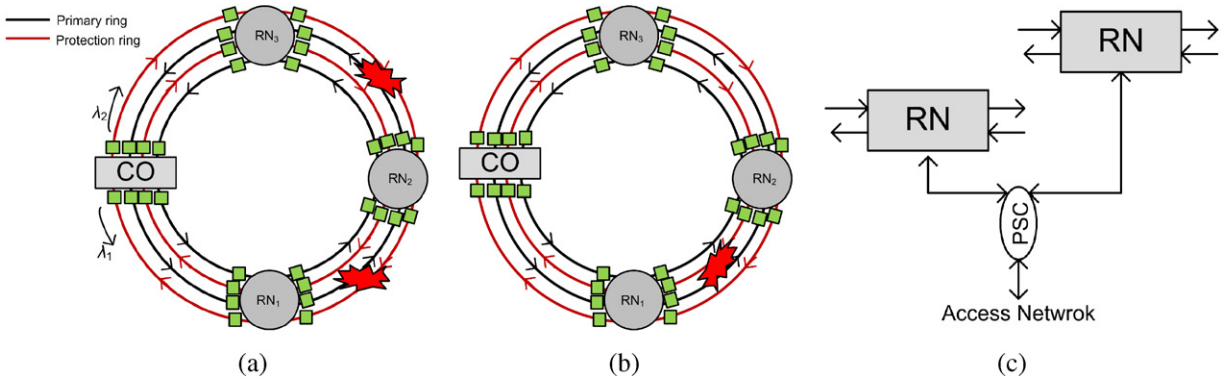

Fig. 6. (Color online) Double-ring pairs LR-PON protection (OCs shown in squares).

discussed three ring protection architectures. Since the main change in these architectures occurs in the ring, we conclude this section by comparing the cost and unavailability for the ring only. Note that all the networks have the same capacity. Four common hypotheses are assumed: (1) N is even, where N is the number of links (fiber segments) in the network; (2) all links have equal availability; (3) all OADMs have equal availability; and (4) the termination node is in the middle of the ring. Under these conditions, we find the cost and unavailability for each network as listed in Table II. C_S and U_S in Table II, respectively, represent the cost and unavailability for the single bidirectional ring protection architecture. The steps of deriving these expressions are given in Appendix A. It is seen that the cost approximately doubles with the number of rings. The unavailability, however, depends on the number of working paths. In a single bidirectional ring, we have two working paths. In a double ring, the number of working paths has been increased to three: the inner ring path, the outer ring path, and the path composed by the two rings in case a double fault occurs on both rings as discussed in Subsection III.B and Fig. 5. The number of working paths can increase to ten if double-pairs ring protection architecture is used. These ten paths can be generated by using each ring individually or by using a combination of two rings in case of a double fault, similar to the strategy in the double-ring protection scheme.

Note that if the RFs are installed on the same duct, all protection architectures may provide the same availability. This is because there is a probability that all fibers in the duct are damaged at the same time. Hence, it is required that the primary and the protection rings be duct disjoint [13].

TABLE II
COST AND UNAVAILABILITY FOR RING PROTECTION ARCHITECTURES

	Cost	Unavailability
Double ring	$\approx 2C_S$	$\approx U_S^{1.5}$
Double-pairs ring	$\approx 4C_S$	$\approx U_S^{5}$

IV. PHYSICAL LAYER FAULT MANAGEMENT SYSTEM

A. Network Management System Principle and Operation

The NMS proposed in this paper has the capability to detect and localize any fault occurring in the ring and then to suggest the suitable protection procedure to recover the network. This NMS uses distributed optical passive monitors such as mirrors, fiber Bragg gratings (FBGs), and optical encoders. These monitors can be designed to reflect a specific wavelength or a subband of the U-band recommended by the ITU-T L.66 recommendation for troubleshooting, surveillance, and monitoring purposes.

Passive optical encoders are one type of passive monitor that combine two functions at the same time: coding and reflection. These intrinsic functions mainly (1) enable scalability for network extensions, (2) allow distinguishing between two or more faults colocated the same distance from the CO, (3) provide centralized automatic and real time monitoring from the CO, and (4) make practical demarcation between network segments. The performance of these passive optical encoders has been studied extensively in [14,15] and demonstrated practically in [16] for standard tree architecture PON monitoring.

The operation of the NMS is based on installing optical encoders at the end of each fiber segment between two RNs. In normal mode, as shown in Fig. 4(a), the NMS sends a monitoring pulse with duration T_s and wavelength λ_1 from the CO in the counterclockwise direction (west). An optical encoder is placed at the end of each ring segment. Each optical encoder will generate and reflect a code by coupling a part of the monitoring pulse. This reflected code will be received at the CO from the west and then decoded to determine the specific ring segment status.

When a fault occurs as shown in Fig. 4(a), the optical code OC_6 is missed at the CO, and then an alarm is generated by the NMS. This alarm signal will control the switches to transmit and receive for RN_3 through the east, and transmit and receive data from RN_1 and RN_2 on the west. This allows successful recovery from the fault. However, the fault between RN_2 and RN_3 will block the monitoring pulse from propagating to RN_3 and then to the CO. Under this condition, the ring becomes divided into two parts: one from the CO to the fault (west) is monitored by λ_1, and the other part from the fault to the CO (east) is not monitored. If a second fault in the second part (east

part) of the ring as between RN_3 and the CO occurs, the NMS cannot detect it. Hence we propose to send a second monitoring pulse carried by a different wavelength (λ_2) on the east to continue monitoring the ring after the first fault is detected. Note that we use a different wavelength λ_2 instead of λ_1 for the second monitoring pulse. This is because using the same wavelength for both monitoring signals will cause part of the generated code to enter the subsequent encoders located in its propagation path rather than completely propagating toward the CO. In other words, dual wavelengths are needed to ensure complete orthogonality between east and west codes.

In the CO, when the code is received and detected, an electronic correlation/decoding function searches for an autocorrelation peak in the decoded signal. If the peak is greater than a threshold, the NMS will assume that the ring segment assigned to this code is healthy; otherwise it declares an alarm and initiates the protection mode. However, sometimes the fault cause is not the ring segment but the RN itself, for example, if RN_1 in Fig. 4(a) is faulty. Then the NMS will interpret this as a fault in the ring segment between RN_1 and RN_2. To solve this problem, we place a different optical encoder after each RN so that we can determine the exact source of a fault. If no code is received from this new encoder, then we decide that RN_1 is faulty.

For double-ring and double-pairs ring protection architectures, optical encoders are installed on each ring to completely monitor the network. The optical encoders in each ring are similar to those in the other rings but operate on different wavelengths. In a fault case, each ring will use two different wavelengths. This means four wavelengths ($\lambda_1 - \lambda_4$) for the double-ring protection and eight wavelengths ($\lambda_1 - \lambda_8$) for the double-pairs ring protection. However, only two wavelengths (λ_1, λ_2) are sufficient for all the rings of these two architectures, at the expense of increasing interference.

B. Encoder Design

Sending two monitoring pulses, with two different wavelengths in opposite directions, through the ring requires the design of a novel type of optical encoder that has the ability to generate and reflect a code toward the CO from any of both directions. We call these encoders symmetrical optical encoders (SOEs). The symmetric property comes from the fact that the codes generated from both sides have the same patterns in time but are carried by different wavelengths. In this paper, we develop two novel types of SOE. To the best of our knowledge, symmetry is a property which has not been addressed in the literature, probably because most (or all) previous research focused on tree monitoring and did not address the ring.

1) FBG-SOE Encoder: Figure 7 shows the FBG-SOE, which is an enhanced implementation of the dual grating asymmetric encoder of [16]. We also show in insets the transfer function of each Bragg grating. The first from the left is a 38% reflector of λ_1 and passes all other wavelengths. The second grating is a double wavelength (λ_1 and λ_2) 100% reflector. This serves for the generation of a code carried by λ_1 in the left and a second code carried by λ_2 in the right. The third grating is a 38% reflector of λ_2 only.

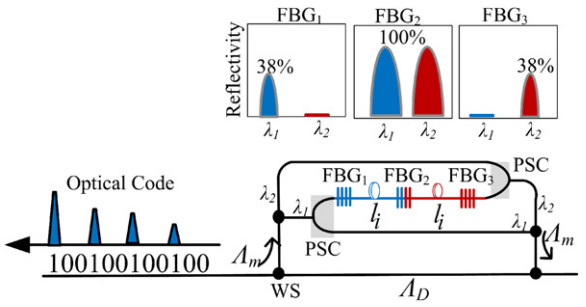

Fig. 7. (Color online) FBG symmetrical optical encoder (FBG-SOE).

When the received monitoring pulse arrives at the encoder input, a wavelength selector is used to separate the data from the monitoring waveband. The monitoring pulse coming from the west with wavelength λ_1 will enter the SOE from the left; the PSC will then couple a part of the monitoring pulse to FBG_1. The remainder of the monitoring pulse will be coupled to the right of the PSC and propagates to the subsequent SOE. In Fig. 6, when the monitoring pulse arrives at the 38% FBG_1, a part of the pulse will be reflected, creating the first subpulse of the code. The remainder of the pulse will propagate through the patch cord that has a length l_i and then be reflected back by 100% FBG_2. The reflected pulse will create the second subpulse of the code when it arrives at the 38% FBG_1. This process continues to produce a multilevel periodic code with a period proportional to the patch-cord length. The generated code will be reflected back to the CO in the clockwise direction. The second monitoring pulse carried by the wavelength λ_2 that is transmitted through the east when a fault occurs will undergo a similar process, except this occurs on the right side. The generated codes then propagate back in the counterclockwise direction to the CO. To distinguish the generated codes, the patch cord between the FBGs is chosen with a specific length for each encoder. This length is given as

$$l_i = T_s c p_i/2, \tag{12}$$

where T_s is the pulse duration, $c \approx 2 * 10^8$ m/s is the light speed in the fiber, and p_i is the repetition period length. For example, the third generated code is represented logically as $OC_3 = 100100100100$. This code has repetition period $p_i = 3$; hence its ring length is $l_3 = 30$ cm for $T_s = 1$ ns. For 32 RNs and using the same probe pulse duration, the longest encoder has a patch-cord length equal to 320 cm (3.2 m). This patch-cord's length will produce a code with time duration in microseconds. This time can be ignored when we compare it with the delay produced by the ring length (see Section VI), which is in milliseconds.

2) Ring-SOE Encoder: This encoder is an enhanced implementation of the setting prepared in [17]. This encoder uses two rings, two couplers and an FBG with 100% reflectivity as shown in Fig. 8. Both rings have length l_i as shown in Fig. 8, where i denotes the i^{th} encoder. This encoder is similar to the FBG-SOE in operation, but differs in the method of code generation. When a part of the monitoring pulse coming from the west carried by λ_1 arrives at the ring, the coupler divides it

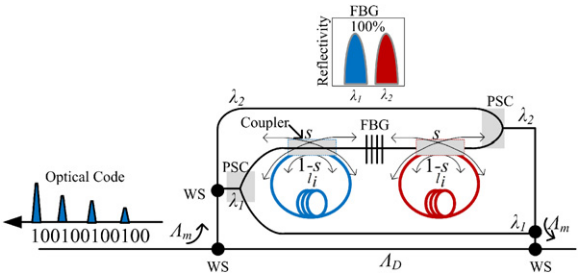

Fig. 8. (Color online) Ring symmetrical optical encoder (Ring-SOE).

into two parts; one propagates toward the FBG, and the other turns inside the ring.

The power splitting ratio s determines the amount of power coupled to the ring and that passed toward the Bragg grating. In extreme but unrealistic cases, when s is one, no power is coupled to the loop, and the code will be only one pulse; when s is zero, all power will be coupled to the loop, and no code will be generated. Realistic cases correspond to s such that $0 < s < 1$. The part that is coupled to the loop will continue to observe other splits while traversing the coupler. Theoretically, this splitting will continue infinitely, generating an infinite-length decaying sequence. The first subpulses in the sequence have the higher power level, and the code can be truncated to the first w subpulses that become the weight of the code. This encoder theoretically operates as a 100% mirror, since all the incident power is reflected by the FBG. The generated code will be reflected back to the CO in the clockwise direction. The ring length for each encoder is given as

$$l_i = T_s c p_i. \tag{13}$$

In the following, we address the deployment strategy of the proposed symmetrical coding-based NMS in single and double-ring protection architectures.

V. Physical Layer Fault Detection, Localization, and Protection Algorithms

The process of network protection begins with fault detection and localization by the NMS. Then an alarm is generated and a control signal is used to initiate the protection mode. However, this process needs a guide to show how to recover from a fault and how to go back to the normal mode after the fault is repaired. In the following we develop two algorithms for unidirectional ring and double-ring protection. These algorithms are to be executed by the NMS and have the ability to detect and localize any fault in the ring. Moreover, they generate alarms showing the location of the fault to initiate a suitable protection procedure to recover from the fault.

A. Single Bidirectional Ring Protection Algorithm

Figure 9 shows the flow chart implemented by our NMS for the single bidirectional ring protection scheme. When a fault occurs, this flow chart leads first to a loss of code (LOC) alarm and then a suitable protection and recovery procedure. We define $C = \{\mathrm{OC}_i\}$, $i = 1,\ldots,M$, as the set of M optical codes in the ring. We also define $R = \{\mathrm{RN}_i\}$, $i = 1,\ldots,K$, as the set of K RNs.

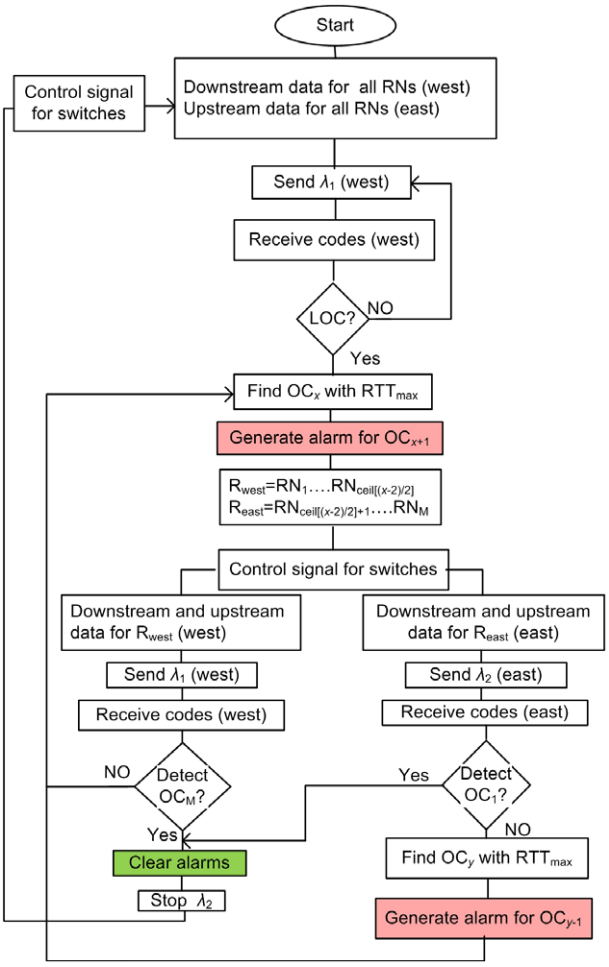

Fig. 9. (Color online) LOC detection, localization and protection algorithm for single bidirectional ring protection.

In normal mode, the downstream data are sent from the west and the upstream data received from the east. The monitoring pulse carried by λ_1 is transmitted from the west and hits the encoders sequentially, generating back a sequence of codes, each of them identifying a specific location in the network. The NMS continuously searches for the farthest OC_x existing in the received signal, i.e., the one with maximum round-trip time ($\mathrm{RTT}_{\max}$). If $\mathrm{OC}_x = \mathrm{OC}_M$ (OC_M is the farthest code observed from the west), this means there is no fault, and the NMS sends a second monitoring pulse to check the network again. If the NMS did not receive OC_M, it determines OC_x (farthest code observed from west), which represents the boundary between the working (west) and faulty (east) parts of the ring. Then the NMS generates an alarm for the OC_{x+1} and switches to the protection mode. In this mode, the NMS controls the switches to transmit and receive data for $R_{\mathrm{west}} = \{\mathrm{RN}_1, \mathrm{RN}_2, \ldots, R_{\mathrm{ceil}[(x-2)/2]}\}$[1] on the west and $R_{\mathrm{east}} = \{\mathrm{RN}_{\mathrm{ceil}[(x-2)/2]+1}, \ldots, \mathrm{RN}_K\}$ on the east. Simultaneously, the NMS sends (in addition to the monitoring signal carried by λ_1) another monitoring signal carried by λ_2 from the east, because

[1] ceiling$(x) = \lceil x \rceil$ is the smallest integer not less than x.

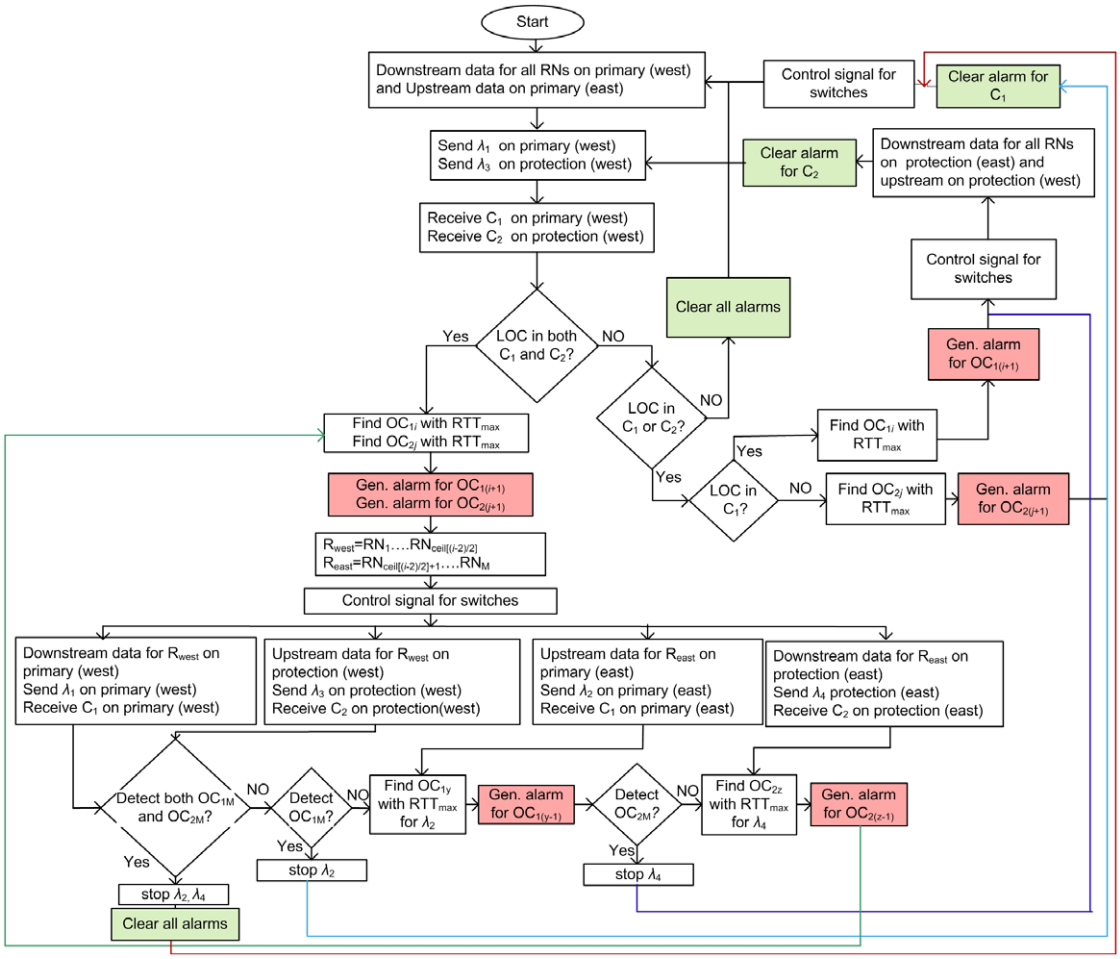

Fig. 10. (Color online) LOC detection, localization and protection algorithm for double-ring protection architecture.

this part of the ring is no longer monitored owing to the fault. The codes of the east path are received from the east.

For the new received OCs from the west, the NMS continuously searches for OC_M. If not detected, the fault is still unfixed, or there is another fault in the ring, then the NMS searches again for the OC with $\mathrm{RTT}_{\max}$. If OC_M is detected, this means that the fault is repaired, and the system can go back to normal mode after clearing the alarms and stopping λ_2. For OCs received from the east, the NMS searches for OC_1 (i.e., the farthest code observed from the east). If this code is detected, the alarm is cleared, and λ_2 is stopped; otherwise the NMS searches for the farthest received OC_y code and then generates an alarm for OC_{y-1}. The two alarms for OC_{x+1} and OC_{y-1} will be like a boundary for the faulty segment(s) or RN within the ring. After moving to the protection mode, the network operator should dispatch technicians to the fault location, where an optical time domain reflectometer (OTDR) is used to determine the exact place of fault within the segment.

B. Double-Ring Protection Algorithm

The double-ring protection flow chart is shown in Fig. 10. We define two sets of OCs for both rings, $C_1 = \{\mathrm{OC}_{11}, \mathrm{OC}_{12}, \ldots, \mathrm{OC}_{1M}\}$ for the primary ring and $C_2 = \{\mathrm{OC}_{21}, \mathrm{OC}_{22}, \ldots, \mathrm{OC}_{2M}\}$ for the protection ring, where $\mathrm{OC}_{i,j}$ represents the j^{th} encoder of the primary ring if $i = 1$ and the protection ring if $i = 2$. In normal mode, the primary ring is used where the downstream data signals for all RNs are transmitted on the west and the upstream data are received from the east. Similarly, a monitoring signal with wavelength λ_1 is transmitted through the primary ring on the west, and a monitoring signal with wavelength λ_3 is transmitted through the protection ring on the west.

When a fault occurs on the primary ring, the NMS detects a LOC from the set C_1, declares an alarm, and then switches the data to the protection ring. Once this fault is repaired, the NMS goes back to normal mode after clearing the alarm. When two faults occur for both rings between two RNs, the NMS detects LOC from both sets C_1 and C_2. At this moment the NMS will localize the place of the faults on both rings and start the recovery process by using both rings to transmit and receive data for all RNs. The downstream for R_{west} is transmitted on the primary ring (west) and its upstream is received on the protection ring (west). The downstream for R_{east} is transmitted on the protection ring (east), and the upstream is received on the primary ring (east). Also, the NMS uses two other monitoring signals: one is transmitted on

the primary ring (east) carried by wavelength λ_2, and one is transmitted on the protection ring (east) carried by wavelength λ_4. These two additional monitoring signals will cover the two parts of the rings after fault location. Once a fault is fixed on any ring, the associated monitoring signal with wavelength (λ_2 or λ_4) is stopped, and the fault alarm for the fixed ring is cleared. This ring will be used then to carry the data. If both rings are repaired, the NMS will stop transmitting (λ_2 and λ_4), clear all the alarms, and go back to the normal mode.

VI. Upper Bound Notification and Recovery Times

A very short disruption of service caused by a physical layer fault in the ring may lead to a very high data loss due to the high data rates, increased wavelength numbers, and customer density. Recovering from this fault and fixing the problem is very important. The endeavor is focused on reducing the fault detection time. Because the NMS system is centralized, the fault detection and localization is performed in the CO. The notification time is defined as the time elapsed between a failure in the physical layer of the network and the localization of the fault by the NMS.

The NMS sends a monitoring pulse from the CO and waits for the received code. After detecting the code, the NMS sends the next monitoring pulse. This procedure is called stop and wait. To decease the time of notification, the transmitted pulses can be pipelined so that pulses are transmitted without waiting for the last code to be received in the CO. To avoid overlapping of the same code from two successive transmitted pulses, we send the pulses with time delay T_c, where T_c is the code duration. This ensures that the next pulse will arrive at the encoder input after the code generated by the previous pulse has left. Hence the upper bound notification time is given as

$$T_N \le \mathrm{RTT}/2 + T_c + T_p, \tag{14}$$

where RTT is the round-trip time that a monitoring pulse takes to cross the ring forward and backward, and T_p is the processing time taken by the NMS to decode, localize, and generate an alarm. The RTT is the dominant factor, which is given in milliseconds, whereas the processing and code duration times have smaller durations (microseconds). The generated alarm will initialize the recovery process. The recovery time is the time taken by the system to recover from a fault. This time depends on the type of switches used in the OLT. If optoelectronic switches are used, they take about 10 ms to switch, which is much slower than electronic switches, which have switching times in nanoseconds. Also, the price of electronic switches is 10 times lower than that for optical switches. Hence we suggest using electronic switches in the OLT. The upper bound recovery time is given as

$$T_R \le T_N + T_{sw}, \tag{15}$$

where T_{sw} is the time delay of the switch. Hence, for electronic switches, the recovery time is dominated by the RTT. Figure 11 shows the simulation results for the recovery time as a function of the fault location in a 100 km long ring. We assumed that there are 32 equidistant RNs and monitoring pulse durations

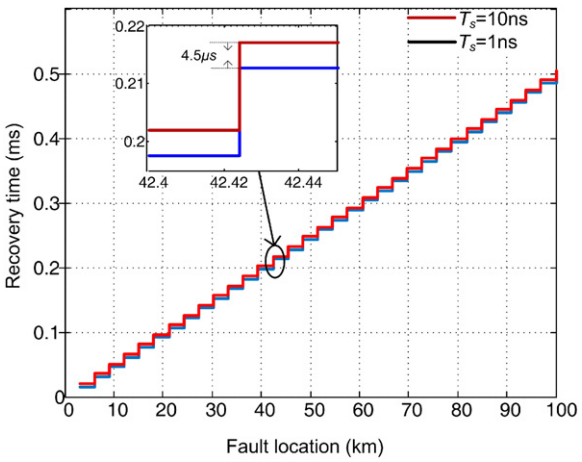

Fig. 11. (Color online) Recovery time versus fault location.

of T_s = 1 ns and 10 ns. We considered the processing and switching times because they are negligible compared with the RTT and code duration. The results show that using wider monitoring pulses, from 1 to 10 ns, will increase the recovery time by 4.5 μs. The simulation also shows that the maximum recovery time is about 0.5 ms for a code located at the end of the ring, i.e., 100 km apart from the CO. This time represents the duration of a one-shot measurement. To improve the fault detection, signal averaging is necessary to reduce the noise effect. This is achieved by taking the measurement many times. However, the recovery time will increase accordingly.

VII. Conclusion

This paper has introduced a physical layer fault management and protection solution for LR-PON based on passive optical coding. We discussed the availability of this network versus the cost and found that protecting only the ring by duplication can reduce the cost of LR-PON by almost half compared with full duplication with high availability. We studied different ring protection architectures used in WDM metro networks to apply them for LR-PON by designing suitable architectures for the RNs and the OLT. We further presented our management system, which is based on optical coding. Two novel optical encoders are designed for this purpose. Moreover, we developed two algorithms for fault detection, localization, and protection executed by the NMS. Finally, we found that the system can recover from a fault in less than 0.5 ms for a 100 km long ring.

Appendix A: Unavailability Derivation for Protected LR-PON

A.1. Single Bidirectional Ring LR-PON

As discussed in Section III, the single bidirectional ring LR-PON has two parallel paths between the CO and an arbitrary termination node. In normal operation, the data are transmitted from the west through m links (fiber segments) to an

arbitrary termination node. The unavailability of this path (P_1) is

$$U_{P_1} = 1 - A_{P_1} = 1 - A_{\mathrm{OLT}} \prod_{i=1}^{m} A_{\mathrm{OADM}_i} \prod_{i=1}^{m} A_{\mathrm{FS}_i},$$

where A_{P_1}, A_{OLT}, A_{OADM_i}, A_{FS_i} are the availabilities of path one, the OLT, the i^{th} OADM, and the i^{th} fiber segment, respectively. In the case of a failure on P_1, the signal is transmitted from the east and traverses $N-m$ links to the termination node, where N is the total number of links in the ring. The unavailability of this path (P_2) is

$$U_{P_2} = 1 - A_{P_2} = 1 - A_{\mathrm{OLT}} \prod_{i=1}^{N-m} A_{\mathrm{OADM}_i} \prod_{i=1}^{N-m} A_{\mathrm{FS}_i}.$$

Four common hypotheses are assumed: (1) N is even, (2) all links have equal availability, (3) all OADMs have equal availability, and (4) the termination node is in the middle of the ring. Under these conditions, we find that the unavailability of P_1 is equal to the unavailability of P_2:

$$U_{P_1} = U_{P_2} = U_P = 1 - A_{\mathrm{OLT}} A_{\mathrm{OADM}}^{N/2} A_{\mathrm{FS}}^{N/2},$$

and the total single bidirectional network unavailability is

$$U_S = U_{P_1} U_{P_2} = U_P^2.$$

A.2. Double-Ring LR-PON

For the double-ring LR-PON, we have three parallel paths between the CO and an arbitrary termination node (see Section III). In normal operation, the data are transmitted from the west through the inner ring (P_1) and traverse m links to the termination node. The unavailability of this path is

$$U_{P_1} = 1 - A_{P_1} = 1 - A_{\mathrm{OLT}} \prod_{i=1}^{m} A_{\mathrm{OADM}_i} \prod_{i=1}^{m} A_{\mathrm{FS}_i}.$$

In the case of a fault in the inner ring, the outer ring is used to transmit data from the east through $N-m$ fiber segments to the termination node. The unavailability of this path (P_2) is

$$U_{P_2} = 1 - A_{P_2} = 1 - A_{\mathrm{OLT}} \prod_{i=1}^{N-m} A_{\mathrm{OADM}_i} \prod_{i=1}^{N-m} A_{\mathrm{FS}_i}.$$

If a double fault occurs on both rings, as shown in Fig. 5(a), both rings are used, the inner ring for downstream and the outer ring for upstream (see Section III). The unavailability of this path (P_3) is

$$U_{P_3} = 1 - A_{P_3} = 1 - A_{\mathrm{OLT}} \prod_{i=1}^{m} A_{\mathrm{OADM}_i} \prod_{i=1}^{m} A_{\mathrm{FS}_i}.$$

With the same assumptions as for a single bidirectional ring, the unavailability of the three paths becomes equal, where

$$U_{P_1} = U_{P_2} = U_{P_3} = U_P = 1 - A_{\mathrm{OLT}} A_{\mathrm{OADM}}^{N/2} A_{\mathrm{FS}}^{N/2},$$

and the total network unavailability is

$$U_D = U_{P_1} U_{P_2} U_{P_3} = U_P^3 = U_S^{3/2},$$

where U_s is the single bidirectional LR-PON unavailability.

A.3. Double-Pairs Ring LR-PON

A similar analysis as applied to the double-ring protection network. We can find 10 paths in this network. Each ring itself represents one path (the total is four paths). The unavailability for each path is equal to U_{P_1} in the double-ring network. In addition, in case of a double fault, two rings can be used for data transmission, similar to a double fault in the double-ring network. Hence, we have the following six pairs of rings: {(1,2), (1,3), (1,4), (2,3), (2,4), (3,4)}. The unavailability of each of these six paths is equal to U_{P_3} in the double-ring network.

Hence, the total is 10 parallel paths. Using the same assumptions as in a single bidirectional ring, the total network unavailability is

$$\begin{aligned} U_{DP} &= U_{P_1} U_{P_2} U_{P_3} U_{P_4} U_{P_5} U_{P_6} U_{P_7} U_{P_8} U_{P_9} U_{P_{10}} \\ &= U_P^{10} = U_S^{10/2}, \end{aligned}$$

where U_s is the single bidirectional network unavailability.

Acknowledgments

This research is supported by The National Plan for Science and Technology (NPST) program through King Saud University, Saudi Arabia, Project Number 09-ELE855-02. The authors acknowledge Prince Sultan Advanced Technologies Research Institute (PSATRI) and the KACST-Technology Innovation Center (RFTONICS) of King Saud University for access to their facilities.

References

[1] H. Song, B. Kim, and B. Mukherjee, "Long-reach optical access networks: A survey of research challenges, demonstrations, and bandwidth assignment mechanisms," *IEEE Commun. Surv. Tutorials*, vol. 12, no. 1, pp. 112–123, Oct. 2010.

[2] R. Davey, D. Grossman, M. Rasztovits-Wiech, D. Payne, D. Nesset, A. Kelly, A. Rafel, S. Appathurai, and S.-H. Yang, "Long-reach passive optical networks," *J. Lightwave Technol.*, vol. 27, no. 3, pp. 273–291, Feb. 2009.

[3] B. Schrenk, J. A. Lazaro, D. Klonidis, F. Bonada, F. Saliou, V. Polo, E. T. Lopez, Q. T. Le, P. Chanclou, L. Costa, A. Teixeira, S. Chatzi, I. Tomkos, G. M. Tosi Beleffi, D. Leino, R. Soila, S. Spirou, G. de Valicourt, R. Brenot, C. Kazmierski, and J. Prat, "Demonstration of a remotely dual-pumped long-reach PON for flexible deployment," *J. Lightwave Technol.*, vol. 30, no. 7, pp. 953–961, Apr. 2012.

[4] ETRI, "WDM-E-PON (WE-PON)," *Working Documents*, 2007.

[5] M. Maier, *Optical Switching Networks*, 1st ed. New York: Cambridge University Press, 2008.

[6] J. Santos, J. Pedro, P. Monteiro, and J. Pires, "Long-reach 10 Gbps Ethernet passive optical network based on a protected

ring architecture," in *Optical Fiber Communication Conf. and the Nat. Fiber Optic Engineers Conf. (OFC/NFOEC)*, San Diego, CA, 2008, pp. 1–3.

[7] H. Song, D. Seol, and B. Kim, "Hardware-accelerated protection in long-reach PON," in *Optical Fiber Communication Conf. (OFC)*, San Diego, CA, 2009, pp. 1–3.

[8] D. Seol, E. Jung, and B. Kim, "A simple passive protection structure in a ring-type hybrid WDM/TDM-PON," in *Proc. 11th Int. Conf. on Advanced Communication Technology*, Phoenix Park, South Korea, Feb. 2009, pp. 447–449.

[9] D. Seol, E. Jung, and S. Lee, "Passive protection in a long-reach WDM/TDM-PON," in *Proc. 9th Int. Conf. on Optical Internet (COIN)*, Jeju, South Korea, 2010, pp. 1–3.

[10] W. Grover, *Mesh-Based Survivable Networks: Options and Strategies for Optical, MPLS, SONET, and ATM Networking*. Upper Saddle River, NJ: Prentice Hall Professional, 2005.

[11] J. Chen, L. Wosinska, M. Chughtai, and M. Forzati, "Scalable passive optical network architecture for reliable service delivery," *J. Opt. Commun. Netw.*, vol. 3, no. 9, pp. 667–673, Sept. 2011.

[12] J. Chen and L. Wosinska, "Analysis of protection schemes in PON compatible with smooth migration from TDM-PON to hybrid WDM-TDM-PON," *J. Opt. Netw.*, vol. 6, no. 5, pp. 514–526, May 2007.

[13] H. Zang, S. Ou, and B. Mukherjee, "Path-protection routing and wavelength assignment (RWA) in WDM mesh networks under duct-layer constraints," *IEEE/ACM Trans. Netw.*, vol. 11, no. 2, pp. 248–258, Apr. 2003.

[14] M. M. Rad, H. Fathallah, and L. A. Rusch, "Fiber fault PON monitoring using optical coding: Effects of customer geographic distribution," *IEEE Trans. Commun.*, vol. 58, no. 4, pp. 1172–1181, Apr. 2010.

[15] M. Rad, H. Fathallah, and L. Rusch, "Performance analysis of fiber fault PON monitoring using optical coding: SNR, SNIR and false-alarm probability," *IEEE Trans. Commun.*, vol. 58, no. 4, pp. 1182–1192, Apr. 2010.

[16] M. Rad, H. Fathallah, S. LaRochelle, and L. Rusch, "Experimental validation of periodic codes for PON monitoring," in *Proc. IEEE Globecom*, Honolulu, HI, 2009, pp. 1–7.

[17] M. A. Esmail and H. Fathallah, "Novel coding for PON fault identification," *IEEE Commun. Lett.*, vol. 15, no. 6, pp. 677–679, June 2011.

Maged A. Esmail received his B.E. degree in electronic engineering from Ibb University in 2006 and M.Sc. degree (with first class honors) in electrical engineering from King Saud University in 2011. From 2009 to 2012, he has been with Prince Sultan Advanced Technologies Research Institute (PSATRI) as a researcher. His research interests include fiber-optic communications, multiple access networks, PON and long-reach PON, network management and protection, and sensor networks. He is a Student Member of IEEE and OSA.

Habib A. Fathallah (S'96, M'01) received the B.S.E.E degree (with Honors) from the National Engineering School of Tunis in 1994 and the M.A. and Ph.D degrees in electrical engineering from Laval University, Quebec, Canada, in 1997 and 2001, respectively. He initiated the use of Bragg gratings technology for all-optical/all-fiber coding/decoding in optical CDMA systems. He was the founder of Access Photonic Networks (2001–2006). He is currently with the Electrical Engineering Department, College of Engineering, King Saud University (Riyadh, Saudi Arabia) and is an adjunct professor with the Electrical and Computer Engineering Department of Laval University (Quebec, Canada). His research interests include optical communications systems and technologies, metro and access networks, optical CDMA, PONs and long-reach PONs, FTTH, network monitoring, and hybrid fiber wireless (FiWi) systems. He is a Member of IEEE and OSA.